

Formation mechanisms of processing defects and their relevance to the strength in alumina ceramics made by powder compaction process

N. SHINOHARA, M. OKUMIYA

Ashahi Grass Co., Hazawa, Kanagawaku, Yokohama, Japan

T. HOTTA, K. NAKAHIRA, M. NAITO

Japan Fine Ceramics Center, Mutsuno, Atsutaku, Nagoya, Japan

K. UEMATSU

Department of Chemistry, Nagaoka University of Technology, Nagaoka, Japan

E-mail: uematsu@vos.nagaokaut.ac.jp

With new characterization techniques, the structures of green and sintered bodies were examined in great detail to understand the formation mechanism of potential fracture origins in alumina ceramics made by the powder compaction process. Large pores, which are found at many fracture origins, were formed in green bodies through two mechanisms. One is created from the dimple in the powder granules and the other from inadequate cohesion of the granules. Another potential cause of fracture, the large grains, developed from large particles in the green body. The concentration, especially of large pores was found to be quite high. This is clearly responsible for the moderate strength with high Weibull's modulus of the alumina ceramic examined in this study. © 1999 Kluwer Academic Publishers

1. Introduction

Microstructural defects including large pores and grains govern important properties, such as fracture strength [1]. They are introduced in the microstructure through the production steps, but details of their formation mechanisms, especially for large pores, have remained mostly unclear. This causes major problems not only in the production but also in the application of ceramics. One typical example is the significant unpredictable variation of properties. This is commonly noted in ceramics which are made through apparently the same method, severely damaging their reliability [2]. Although the source of the variation is commonly ascribed to the change in the characteristics of defects, there is often no clear evidence for this explanation. The lack of an adequate tool has been one of the largest difficulties which hinders the clarification of the formation mechanism. The potential tool should be capable of clarifying large defects in powder packing structure of green body, which are believed to be transformed into defects through the firing process. The existing tools, however, are far from satisfactory in detecting a feature of extremely low concentration in the body, which is characteristic of fracture initiating flaws. Even today, the formation mechanisms of defects is mostly imagined through microstructure analysis of sintered ceramics [3]. A direct examination for the formation mechanism is strongly needed.

New characterization tools introduced by the present authors are very promising for directly examining the

structural defects in green bodies [4, 5]. With these tools, green specimens are made transparent with immersion liquids, and their internal structures are observed with various types of optical microscopes in the transmission mode. They have the capability of detecting structures of extremely low concentration, such as potential fracture origins at a resolution of a few microns. These features of the tools are ideal for examining detrimental processing defects and non-uniform packing structures of powder particles in the green bodies. This high potential of the tool is only possible with the transmission mode of examination. With scanning electron microscopy (SEM), which is basically a two dimensional observation, it is extremely difficult to detect these structures. Defects and various unique structures examined with these tools include, binder segregation at the surface of powder granules [6], aggregates of fine powders [7], particle orientation and pores in powder granules [8], crack-like voids at the granules boundaries [9] and particle orientation in compacts [10, 11], etc. In these studies, however, these subjects have been examined separately, and even on different substances in some cases. For examining sintered ceramics, the similar optical microscopy can be applied and was again found to be very powerful in the characterization of potential fracture origins [12]. Thin ceramics are transparent without the immersion liquid, and the structure can be examined in great detail with transmission optical microscopy. This technique has been used in the past for ceramics [13]. With these tools, it may be

of great interest to examine the formation mechanisms of defects systematically for a system commonly used in fundamental research as well as in industry.

The objective of this paper is to clarify the formation mechanism of large processing defects such as large pores and grains in the production process of ceramics by using these new characterization tools. As a typical example, commercial alumina ceramics called Refereeram made from a powder of typical industrial grade has been studied. The processing is well controlled and is quite reproducible. It provides an opportunity for clarifying the structural relationship for defects which are present in powder granules, compacts made from them and resultant ceramics, systematically. Specific features focused on in this study are large pores and particles. Also the orientation of powder particles was noted in various steps of the processing. These may have a significant effect on the microstructure development and the resultant properties. Details of the subject, however, will not be treated in this paper. Nevertheless, the results obtained in this paper are very unique and will contribute significantly to a better understanding of the processing of ceramics as well as to the development of ceramics with improved performance.

2. Experimental

Details of specimen preparation have been published elsewhere [14]. Table I shows the raw materials and their amounts used in this study. An outline of the procedure for sample preparation is as follows. The powder was mixed with the dispersant and distilled water for 2 h by stirring. The slurry obtained was then ground by passing it once through an attrition mill operating with alumina grinding media (2 mm diameter) at 900 rpm and a feeding rate 600 ml/min. After passing through a 37 μm sieve, binder and lubricants were added, and then the slurry was stirred for 15 h. The slurry was spray dried with the inlet and outlet temperatures 150 and 70 $^{\circ}\text{C}$, at the feeding rate of 300 ml/min. Granules (400 g) were uniaxially pressed in a square die (125 \times 125 mm) at the applied pressure 9.8 MPa, and then cold isostatically pressed at 176 MPa. The green bodies were placed in an electrical furnace and sintered at 1590 $^{\circ}\text{C}$ for 2 h in air.

The structures of granules and green bodies were examined with the liquid immersion method. In the structural examination of granules, they were placed on a

TABLE I Materials used for experiments

Material	Producer	Product name	Remarks
Alumina powder	Sumitomo Chemical	AES-11E	Highly sinterable low soda alumina
Dispersant	Chukyoyushi	Seruna D-305	Ammonium polyacrylate
Binder	Chukyoyushi	Seruna WF-804 + Seruna WF-610	Wax type
Lubricant	Chukyoyushi	Serosol 920	Emulsion of stearic acid

glass slide and a few drops of 1-bromonaphthalene were added to make them transparent. The green body was thinned to a tenth of a millimeter with grinding paper for examination. A few drops of the same liquid and methyleneiodide were added for microscopic observation in the normal and crossed polarized light modes, respectively. The structures of the ceramics were examined also using thinned specimen. Requirements for the examination in this case are; the thickness is less than about 50 μm and both faces must be finished with diamond paste of 0.5–2 μm . The specimen has high transparency at this thickness, and no immersion liquid is needed in the examination.

The particle size distributions in the slurry were measured with a laser diffraction particles size analyzer (Mastersizer, Marburn) before and after the grinding. The size distribution of granules was measured with sieves. The pore size distribution was examined with mercury porosimeter (Model 220, Calro Elba, Italy). The fracture strength was determined with 4-point bending method, with the outer and inner spans 30 and 10 mm, respectively. The surface of the specimen was finished with a diamond grinding wheel #800. An universal testing machine was applied with the cross head speed 0.5 mm/min. The fractured surface was examined with SEM.

3. Results

Fig. 1 shows the particle size distributions of the raw and ground powders. Almost the same particle size distribution was found for them, showing that the short grinding used in this study had no significant influence on the particle size. In both powders, the size of particle ranged from 0.1 μm to over 7 μm with the average 0.5 μm .

Fig. 2 shows the size distribution of granules determined by sieving. The size of granules varies significantly, ranging 25–150 μm with the average approximately 85 μm . In the range between 40 and 150 μm , the distribution varied almost linearly.

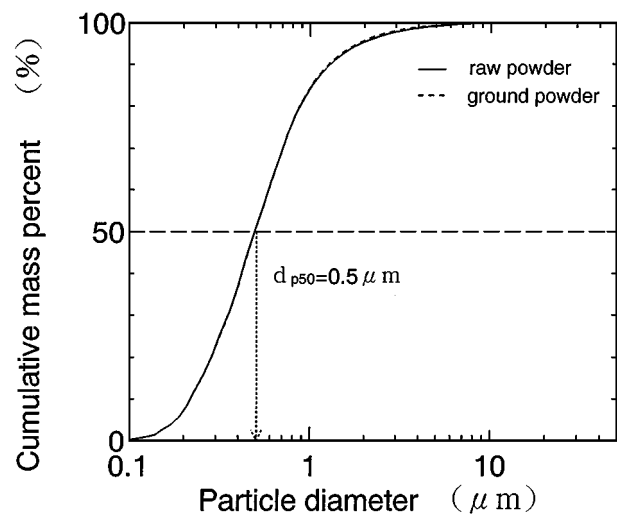


Figure 1 Particle size distribution of raw and ground powders.

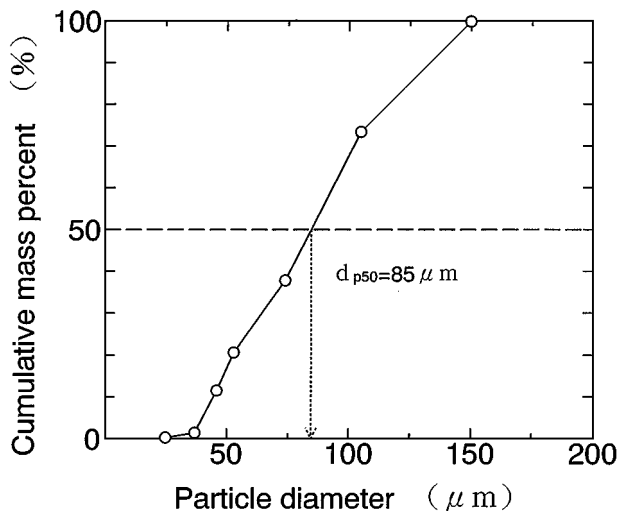


Figure 2 Granule size distribution determined by sieving.

Fig. 3 shows the normal light micrographs of the granules immersed in 1-bromonaphthalene. It clearly shows that all granules, even very small ones, contain dimples. The shape of dimple may not be simple; the diameter varies within the granule. As an average, the diameter and the depth of the dimple are approximately $1/4$ – $1/3$ and $2/3$ of the granule size, respectively. Namely, the fraction of the void space within the granule is not large, against the first impression. By assuming a cylindrical shape, the void space is only approximately 6–11% of the apparent granule volume.

Fig. 4 shows the SEM micrograph of the granules. A wide range of size is noted, which is consistent to the above observation. Most of the granules have irregular shapes with deep dimples. In some granules, however, the dimple was apparently absent. Clearly, they are placed on the specimen holder with the dimple side down.

Fig. 5 shows the normal optical micrographs of a compact after binder removal. Boundaries of granules are clearly visible due to less dense packing of powder particles and are approximately round in the micrograph. Many boundaries consist of mixtures of cracks

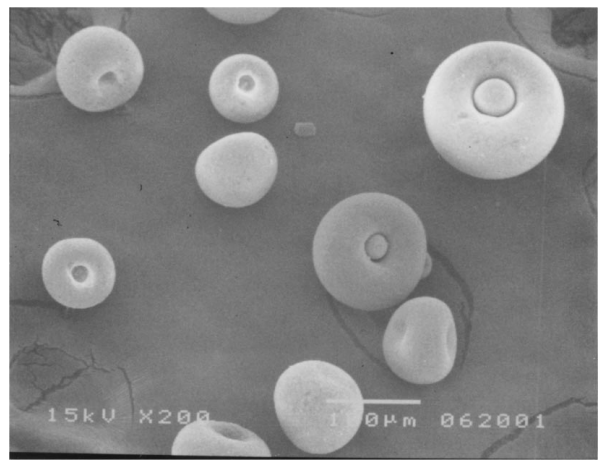


Figure 4 SEM micrograph of alumina granules.

and pores. Sharp cracks are also observed at the centers of granules. These cracks are clearly formed from the dimples in the granules through fracture by compaction. Pores and cracks of large size were only found in these regions in the micrograph and are the major source of large pores and/or cracks in the green body.

Fig. 6 shows the structures of a compact examined, using crossed polarizers in the direction of uniaxial compaction. Two features were noted, i.e. diffuse bright regions and scattered small bright spots. The former areas constitute part of a circle. Inspection in the normal light mode showed that each circle corresponded to the boundary of a granule. The small bright spots changed in brightness with the rotation of specimen at every 45° . They were clearly large alumina particles. At or near the boundaries of granules, large alumina particles are aligned with their maximum face, tentatively assumed to be c-face, along the boundary. With the rotation of the specimen, the brightness of diffuse area also changed at approximately the same angle for the above bright spots. This optical contrast shows that matrix alumina particles in the compacts are also aligned with their c-face parallel to the boundary. A similar structure was noted in a micrograph taken from the direction normal

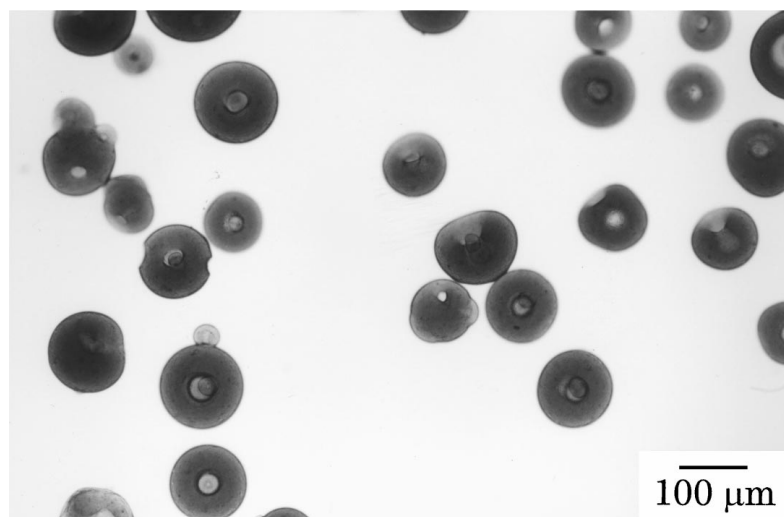


Figure 3 Internal structure of alumina granules observed with the immersion liquid optical microscope of transmission mode.

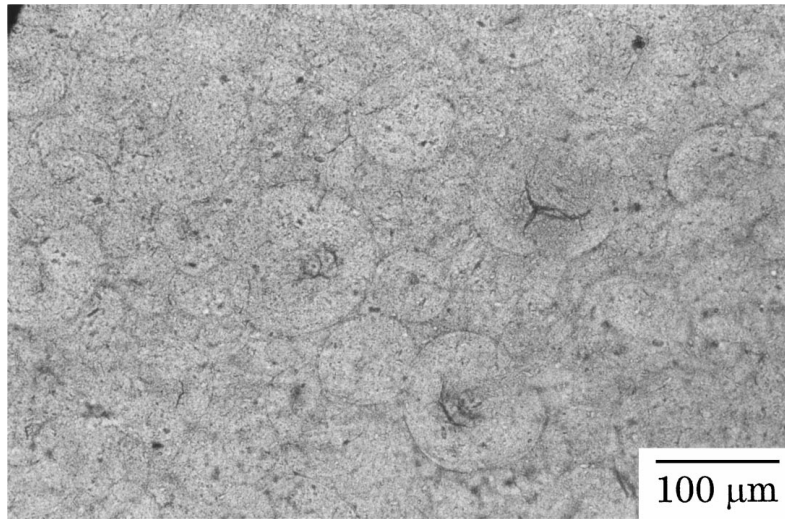


Figure 5 Internal structure of alumina compact observed with the immersion liquid optical microscope of transmission mode.

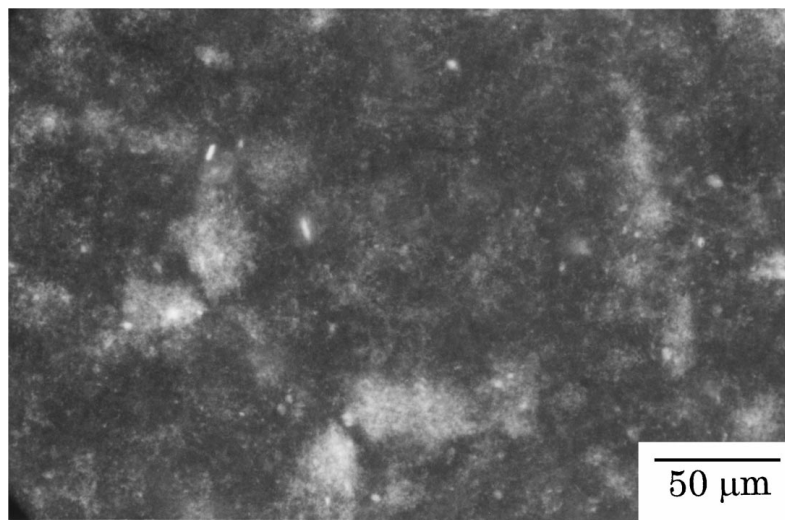


Figure 6 Internal structure of alumina compact observed with the immersion liquid crossed polarized light microscope of transmission mode.

to the direction of uniaxial compaction. However, the circular image of granule boundary was less clear in the micrograph.

Fig. 7 shows the micrographs of the ceramic made from the above green body by sintering. The relative density of the specimen was 98.0%. Many large pores are found in the structure. They are divided into two groups by their shapes. One is pores located at the boundaries of granules and has a narrow crack-like shape. The other appears to be rather round and to be distributed evenly over the specimen. The same area of the specimen was also examined with the metallographic mode of the microscope. It shows that approximately one-fifth of all pores are seen. Some large pores appeared smaller with this microscope, since only a small part of pore is exposed on the surface. The closer examination with the transmission optical microscope shows that the large round pores are located at the center of granules, whenever the boundaries of granules were seen. The origin of these pores is clearly the dimple at the center of granules. The distance between these pores is approximately twice the radius of granules,

50–150 μm , again showing that these pores are formed from the dimples. The origin of pores at the boundaries of granules is clearly the void between granules. The total number of pores at the center of granules is less than that at the boundaries.

Fig. 8 shows the crossed polarized light micrograph of the ceramics. Each grain can be clearly seen. The structure appears to be duplex, consisting of approximately the same fraction of small and large grains. With the rotation of the sample stage, each grain changed its brightness at every 45° . The angle for the change was different for each grain. The crystalline axes are randomly oriented for these grains. The size of the grains estimated from the optical image is much larger than the particles size of the starting powder. Some of the exceptionally large grains were found to be over 30 μm . The origin of these grains must be large particles found in the green body.

Fig. 9 shows the strength distribution of the ceramics. The ceramic has a very high Weibull's modules, 33. However, its strength is moderate, 350 MPa, which is typical of this type of alumina ceramic.

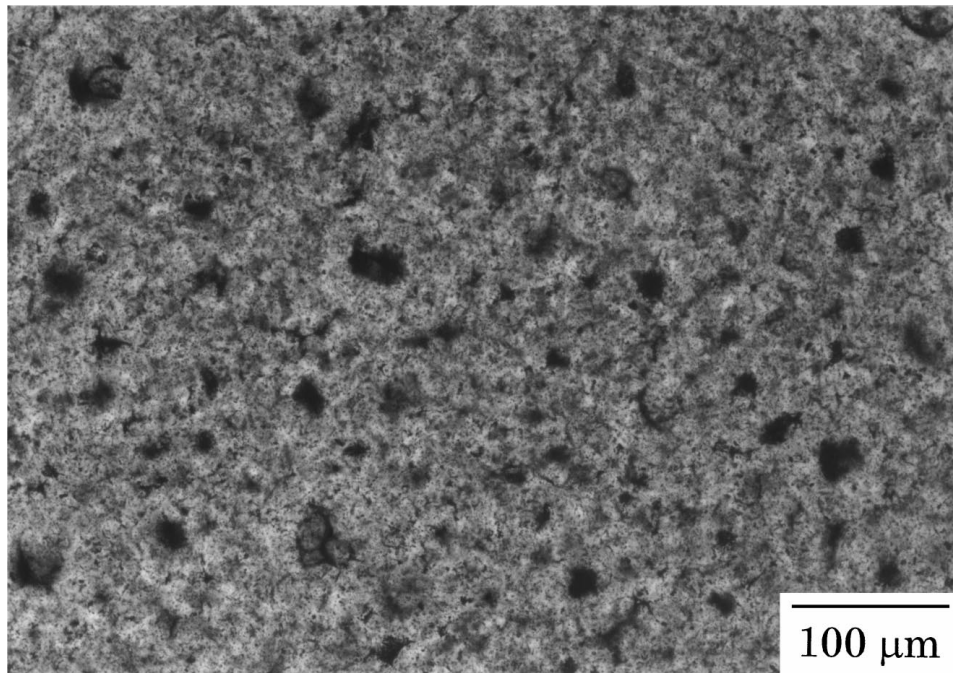


Figure 7 Transmission photomicrograph for alumina ceramics.

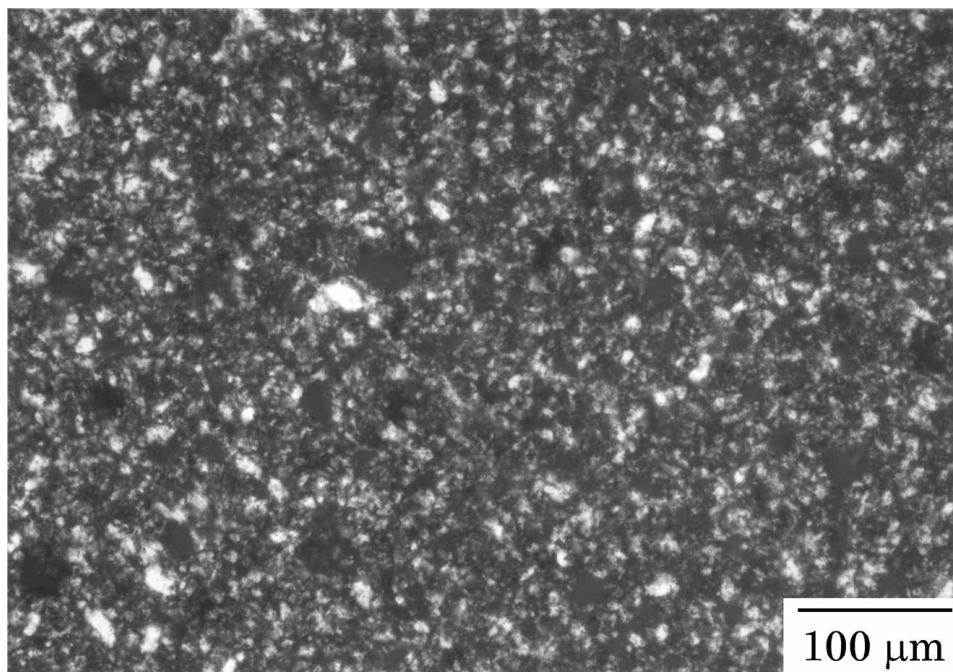


Figure 8 Crossed polarized light micrograph for alumina ceramics.

Fig. 10 shows a SEM micrograph of a fracture origin. Fracture origins in these ceramics were very difficult to find, especially for those of high strength. This micrograph is taken for a specimen of the lowest strength and represents a special case. The void between the granule is clearly the fracture origin in this specimen.

4. Discussion

The formation mechanism of large defects is clarified in this study. Large pores in the present ceramics are made from one of two kinds of large defects in the green body. One is the voids made from the dimples in granules, and the other the boundaries of granules.

Clearly, the dimples leave cracks at the center of deformed granules in the green body even after the isostatic compaction at high pressure. Incomplete cohesion of the granules leaves another crack-like defect at their boundaries. Presence of binder is also responsible for the defects at the boundaries of granules. Other sources of defects are possible to imagine, such as dust particles introduced by chance. However, these appear to be only minor source of large pores in the present system. In fact, an inspection shows that all large pores in Fig. 7 are made from one of the above two major defects in the green body. Large grains, another type of defect, must be formed from large particles in the starting powder through grain growth.

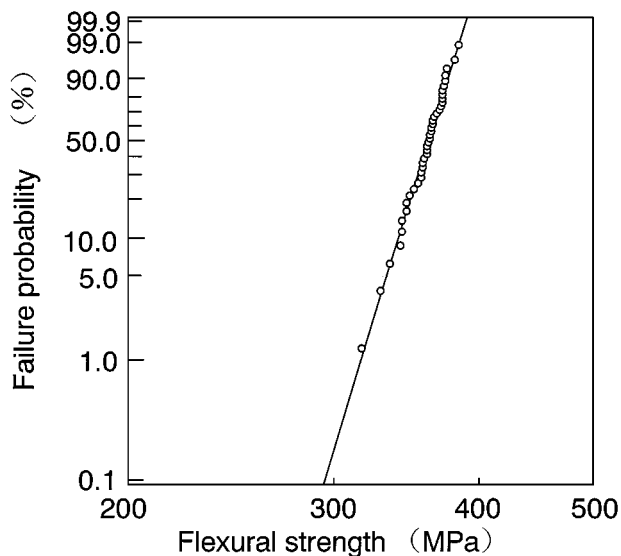


Figure 9 Strength distribution of alumina ceramics.

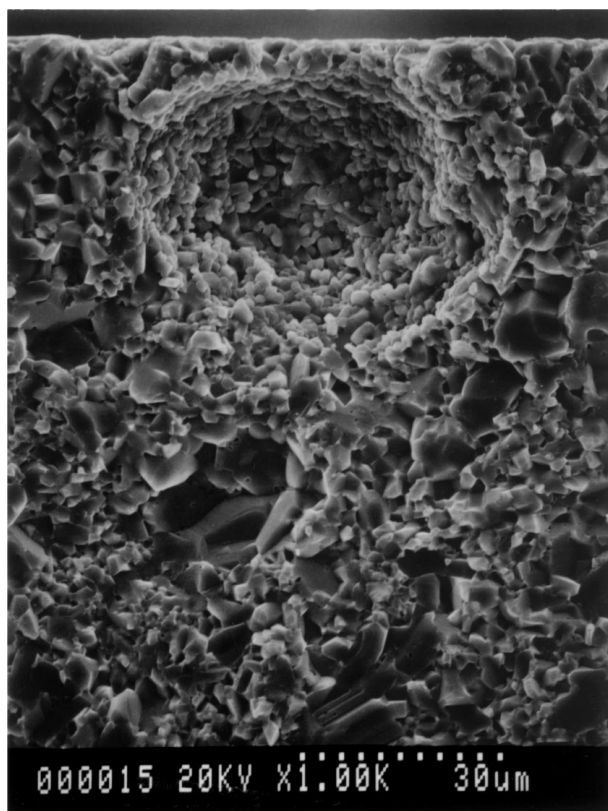


Figure 10 An example of fracture origin in alumina ceramics.

A recent paper reports the formation mechanism of dimples in silicon nitride granules [15] and its influence on densification [16, 17]. The formation of dimples is closely related to the dispersion of powder particles in slurry for spray-drying. Granules with dimples tend to be formed from well dispersed slurry. In addition to the irregular shape, granules made from dispersed slurry are hard and can not be deformed easily. They tend to leave many large defects in green body after compaction as found again in this study. In contrast, flocculated slurries tend to result in soft spherical granules without large pores. They are compacted homogeneously to form a green body with uniform structure.

The defects in ceramics appears to be more distinct than those in the green body. This result is consistent with our knowledge on the behavior of large pores in the densification process. Thermodynamic arguments show that pores larger than a critical size grow in sintering [18, 19]. This was experimentally verified in a recent papers [20, 21]. In these studies, the morphological change associated with densification was followed by repeating the observation and the heat treatment for a large pore which was located inside of an alumina powder compact. The same liquid immersion method of this study was used in that observation. A large crack-like pore was found to grow with the densification process.

The very high concentration of pores in Fig. 7 is only apparent. It does not contradict to the high relative density of the ceramics. The apparent high concentration is ascribed to the unique observation method of the present study, in which pores located at various depth in the specimen are observed simultaneously. This is a clear contrast to the microstructure observed with the conventional analysis, where the observation on polished and etched sections show pores at this level only. Clearly, the present characterization method based on the transmission observation is best suited for examining those features of small concentrations.

One of two types of large pores clearly behaves as fracture origin. Both of them must be removed through better processing. However, it is not certain which of the two types of pores, is more detrimental to the strength of the present ceramics. Fractographs do not provide a clear answer for this subject, although the crack-like pore at the boundary of granule (Fig. 10) is the fracture origin for an extremely weak specimen. Morphologically, a narrow crack tends to be more detrimental for strength than a round pore, since it causes higher stress concentration in the matrix of its immediate vicinity. However, even round pores are detrimental, since sharp cracks with sizes of a few grains accompanies it. The size is also important, since the stress intensity is proportional to the 1/2 power of the size, shape being the same. The size of pores at the center of granules appear to be larger than those at the granule boundaries.

The high Weibull's modulus can be explained by the pore structure in the matrix. The high concentration of pore makes the number and size of pores within the effective volume for fracture similar for all specimens. The strength governed by flaws of similar size and shape should be rather constant. The average strength is expected to be moderate for this material, although the Weibull's modulus should be very high. It is very interesting to make a more detailed analysis on pore size distribution and to predict the strength distribution based on it. This subject will be treated in a separate paper [22].

The local orientation of powder particles is an interesting structure feature of the green body, since it should affect the densification behavior as well as the microstructure development [13]. This subject has been examined for alumina ceramics made by the injection molding process, where the orientation of powder particles is more distinct and simple [23]. In densification,

less shrinkage was noted along the flow direction in the injection molding than the direction normal to it. This phenomenon was explained by the particle orientation along the flow direction, in which elongated particles are aligned with their largest face parallel to the flow direction. In this structure, the shrinkage is less for the direction parallel to the alignment than normal to it. In the present green body, the orientation of particles is locally different and the densification behavior during sintering is expected to vary accordingly. Local stress must be developed in the body after sintering which affects mechanical and various other properties of the ceramics. Further study is clearly needed for the details of local stress and its significance on the properties.

It is generally believed that the large particles grow during the densification process and are one of the potential origins of large grains in the sintered microstructure. These large grains may behave as another fracture origin. The behavior of large particles in the densification process has been examined for alumina ceramics made by an injection molding process [22]. The large particles grew more rapidly than small matrix grains, forming very large grains in the sintered body. This subject is not examined in detail in this study, however, and is also left for further study. Grain growth behavior is complicated in alumina ceramics. Minor impurities are known to affect it significantly [23–25].

In the development of better ceramics, the research methodology presented in this paper should be very important. The approach of this paper is in clear contrast to the conventional practice, in which the quality of the processing is evaluated mostly through the examination of the resultant microstructure and the property measurement of sintered body. The conventional approach is not only very inefficient but also inaccurate. Without understanding the formation mechanisms of defects, only an empirical approach is possible for the improvement of processing, severely retarding the progress of the processing. Lack of understanding is also a large obstacle in the scientific study of processing. With the present methodology, the microstructure and the properties of ceramics can be easily and accurately predicted before the firing stage. It has a potential to open the black box of processing.

References

1. F. F. LANGE, in "Fracture Mechanics of Ceramics," Vol. 1, edited by R. C. Bradt, D. P. H. Hasselman and F. F. Lange (Plenum, New York, 1973) p. 3.

2. *Idem.*, *J. Amer. Ceram. Soc.* **72** (1989) 3.
3. W. D. KINGERY, in "Ceramic Processing Before Firing," edited by G. Y. Onoda and L. L. Hench (Wiley, New York, 1978) p. 291.
4. K. UEMATSU, J.-Y. KIM, Z. KATO, N. UCHIDA and K. SAITO, *J. Ceram. Soc. Japan* **98** (1990) 515.
5. K. UEMATSU, *Powder Technology* **88** (1996) 291.
6. Y. ZHANG, N. UCHIDA and K. UEMATSU, *J. Mater. Sci.* **30** (1995) 1357.
7. K. UEMATSU, J.-Y. KIM, M. MIYASHITA, N. UCHIDA and K. SAITO, *J. Amer. Ceram. Soc.* **73** (1990) 2555.
8. K. UEMATSU, T. TANAKA, Y. ZHANG and N. UCHIDA, *J. Ceram. Soc. Japan* **101** (1993) 1400.
9. K. UEMATSU, M. MIYASHITA, J.-Y. KIM, Z. KATO and N. UCHIDA, *J. Amer. Ceram. Soc.* **74** (1991) 2170.
10. K. UEMATSU, H. ITO, Y. ZHANG and N. UCHIDA, *Ceram. Transaction* **54** (1995) 83.
11. K. UEMATSU, H. ITO, S. OHSAKA, H. TAKAHASHI, N. SHINOHARA and M. OKUMIYA, *J. Amer. Ceram. Soc.* **78** (1995) 3107.
12. K. UEMATSU, M. SEKIGUCHI, J.-Y. KIM, K. SAITO, Y. MUTOH, M. INOUE and Y. FUJINO, *J. Mater. Sci.* **28** (1993) 1788.
13. F. V. DIMARCELLO, P. L. KEY and J. C. WILLIAMS, *J. Amer. Ceram. Soc.* **55** (1972) 509.
14. Japan fine ceramics center, Technical Report, TR-AL1, JFCC, Japan, 1995.
15. H. TAKAHASHI, N. SHINOHARA, M. OKUMIYA, K. UEMATSU, J. TSUBAKI, Y. IWAMOTO and H. KAMIYA, *J. Amer. Ceram. Soc.* **78** (1995) 903.
16. H. TAKAHASHI, N. SHINOHARA and K. UEMATSU, *J. Ceram. Soc. Japan* **104** (1996) 59.
17. Y. IWAMOTO, H. NOMURA, I. SUGIURA, J. TSUBAKI, H. TAKAHASHI, K. ISHIKAWA, N. SHINOHARA, M. OKUMIYA, T. YAMADA, H. KAMIYA and K. UEMATSU, *J. Mater. Res.* **9** (1994) 1208.
18. W. D. KINGERY and B. FRANCOIS, in "Sintering and Related Phenomena" edited by G. C. Kuczynski, N. A. Hooton and C. F. Gibbon (Gordon and D. Breach, New York, 1976) p. 471.
19. B. J. KELLETT and F. F. LANGE, *J. Amer. Ceram. Soc.* **72** (1989) 725.
20. J. ZHENG and J. S. REED, *ibid.* **72** (1989) 810.
21. K. UEMATSU, M. MIYASHITA, J.-Y. KIM and N. UCHIDA, *ibid.* **75** (1992) 1016.
22. M. INOUE, Y. ZHANG, N. UCHIDA and K. UEMATSU, *J. Mater. Res.*, in press.
23. K. UEMATSU, S. OSAKA, N. SHINOHARA and M. OKUMIYA, *J. Amer. Ceram. Soc.* in press.
24. S. J. BENNISON and M. P. HARMER, *ibid.* **68** (1985) C22.
25. C. A. HANDWERKER, P. A. MORRIS and R. L. COBLE, *ibid.* **72** (1989) 130.
26. S. IK and S. BAIK, *ibid.* **77** (1994) 2499.

Received 30 September 1997
and accepted 2 March 1999